

NASA/ASF Project Report

Ref: NRA 94-MTPE-05
NASA Ref: 1995-ADRO00194
RTOP: 665-21-02
ADRO Project ID: 164

“The Circulation and Characteristics of Weddell and Ross Sea Ice”

PI: Mark R. Drinkwater
Jet Propulsion Laboratory
California Institute of Technology

Co-I: David Long
Microwave Earth Remote Sensing Laboratory
Brigham Young University

November 1998

Executive Summary

- To date, from 126 ordered scenes, we have received 35 frames. Of the delivered scenes, we have received 8 standard beam (STD2) frames and 27 non-qualified ScanSAR (SNB) images. All ScanSAR frames are unqualified and have significant mis-location and calibration problems, which have been reported to ASF. All must be reprocessed when Wide Swath beam calibration is completed in summer 1999.
- We have filed 1998/9 DAR's for weekly ScanSAR (SWB) alternative coverage in austral summer and winter to capture some ScanSAR SWB data of our region during formation and melting, respectively. This will enable of delivery of calibrated ScanSAR products within a final year of extended ADRO support.
- Expectations of winter ScanSAR coverage can not be met due to general constraints on OBR usage and annual Radarsat "eclipse" that causes lapse of data below ~60S during late fall and early winter (mid May to late July). Spacecraft eclipse is unfortunate since it excludes viewing the progression in early winter sea-ice conditions and critical open-ocean polynya formation events such as that occurring during May-July 1998 in the Weddell Sea.
- In the absence of accurately calibrated or geolocated ScanSAR images, the existing Radarsat standard beam, ERS-1/2, and J-ERS-1 image catalogs have been exploited. In conjunction with ERS Scatterometer data, SSM/I data and NSCAT data we have:

1. Studied ice motion dynamics and area fluxes at daily intervals throughout 1992
2. studied interannual ice melt signatures from 1992-1997
3. made comparisons of NSCAT and unqualified Radarsat Wide swath products
4. initiated a Southern Ocean ice-classification study using overlapping multichannel data for training samples.

Project Goals

The objective of the study is to continue to use Southern Ocean satellite microwave data (including RADARSAT data) for extracting gridded sea-ice parameters such as drift velocity, divergence, shear and opening/closing. These results will be used in conjunction with combined calibrated active/passive satellite image characteristics to understand the primary seasonal to interannual variability in the Weddell and Ross Seas. Observational data will be used to accurately prescribe boundary conditions in regional model calculations of surface fluxes of heat, salt, freshwater and momentum using the massively parallel OCCAM fine-resolution, coupled ice-ocean-atmosphere model.

Progress in Absence of Radarsat Data

Since calibrated RADARSAT wide-swath frames have not yet become freely available for ice-motion processing, techniques have been developed for gridding and processing radar scatterometer image-derived ice-motion products from ERS-1/2 and NSCAT, SAR data from ERS-1/2, and SSM/I passive microwave radiometer (through collaboration with Jim Maslanik and Chuck Fowler) Gridded ice-motion data sets have been generated and compared from each data source (at 3 and 1 day intervals) for an complete annual cycle in 1992. Coincident field-deployed GPS/Argos buoy and drifting ice camp locations have been used to check on the validity of the tracked drift vectors. Furthermore, temporally and spatially overlapping SAR motion vector grids have been employed for comparative purposes.

Comparisons with ECMWF pressure field data indicate that sea ice drift is forced predominantly by large-scale synoptic pressure fields, and that high frequency motion is driven by passing low-pressure systems and tidal forcing (in continental shelf regions). The latter are significant for new-ice production. Synoptic scale sea-ice drift responds rapidly to changes in forcing on timescales of 12 hours or less depending on the location with respect to the coastline. Seasonality of ice drift is linked to the extent of the sea ice within the Weddell and Ross sea basins and the translation of internal ice stresses through the pack ice.

Sea Ice Dynamics

Since Antarctic ice dynamics data are sparse in contrast to the Arctic basin, a Southern Ocean-wide dataset is a primary requirement to understanding the response of Antarctic sea ice to meteorological and oceanographic forcing. To-date, techniques developed for tracking and gridding low-resolution radar and radiometer ice motion data were employed in this study. ERS and NSCAT Scatterometer, and SSM/I motion products were analysed; (a) one-day gridded SSM/I-tracked motion, and (b) 6-day smoothed SSM/I 1 day motion (for compatibility with the Scatterometer products). ERS and NSCAT ice motion data were computed at 3 day intervals. The comprehensive details of these ice motion products are reported elsewhere in a PoDAG White Paper (Maslanik et al., 1998). The following provide some excerpts of the data attributes pertinent to this ADRO project:

- Antarctic SSM/I data were tracked by Chuck Fowler (CCAR) and then analysed in conjunction with buoy validation data supplied by World Climate Research Program International Antarctic Buoy Program (WCRP-IPAB) participants.
- Scatterometer image data were tracked in conjunction with Ron Kwok using the method described in Kwok et al. (1998).
- ERS-1 data were oversampled by a factor of 4, which yielded a pixel spacing of approximately 2.2 km (consistent with sampling used for 85 GHz SSM/I data).
- Comparisons were made between SSM/I and Scatterometer motion datasets and buoy data, using gridded vectors within 50 km of the buoy reported locations.

Gridded Motion products

Products were compared on a polar stereographic grid projection with the x axis oriented at 90°E and the y axis parallel to the 0° meridian, to facilitate overlaying vector products onto the radar scatterometer images from ERS-1/2 and NSCAT, together with NSIDC passive microwave images and SAR data from ERS-1/2 and Radarsat. Consistent gridded ice motion data sets have been generated from each data source (at 3 and 1 day intervals, respectively) for an entire year in 1992. Vectors were regridded at 10 pixel spacing (where pixel spacing in ERS Scat products is 8.9 km), resulting in gridded vectors at ~90 km intervals. The following describe the principal findings of each type of product:

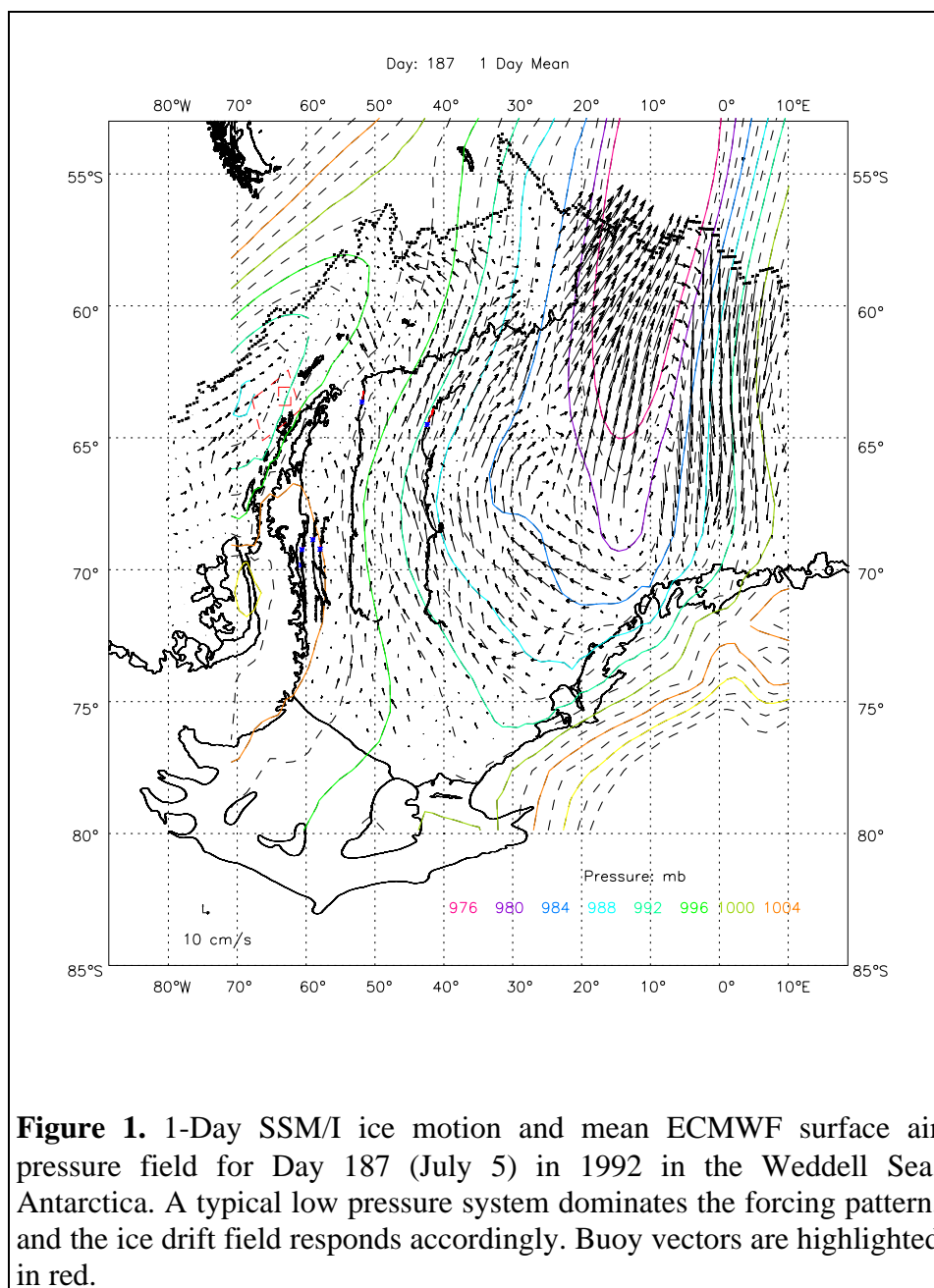


Figure 1. 1-Day SSM/I ice motion and mean ECMWF surface air pressure field for Day 187 (July 5) in 1992 in the Weddell Sea, Antarctica. A typical low pressure system dominates the forcing pattern, and the ice drift field responds accordingly. Buoy vectors are highlighted in red.

SSM/I Motion Data

Comparisons of the CCAR-tracked Antarctic SSM/I ice drift with the buoy drift data indicate errors as follows;

- 1-day rms errors for x and y component displacements were similar at 0.76 pixels (6.7 km) and 0.79 pixels (7.0 km), respectively.
- 1 day rms vector displacement and speed errors are approximately 9.7 km/d and 11.23 cm/s, respectively.

Clearly the rms pixel error is less than the scale of 1 original SSM/I pixel. However, as Kwok et al. (1998) have pointed out, daily ice motion estimates are very noisy. A typical example of SSM/I 1-day motion is shown in Figure 1, in comparison with the mean 24-hour ECMWF surface air pressure field.

Since comparisons between 1 day SSM/I motion with buoy data indicate a Gaussian error distribution and near-zero mean bias, averaging was performed to reduce tracking errors. 6-Day averages of 1-day motions were chosen for investigation since they are most comparable to the tracking products derived using Scatterometer images. As expected, the result indicates that the rms errors decrease approximately in proportion to $1/\sqrt{n}$, when resulting 6-d motion data are compared with the buoy information. The errors for the 6-day mean motion fields are:

- The x and y rms errors are reduced to 4.1 km (4.7 cm/s) and 4.18 km (4.8 cm/s).

This is a significant improvement over 1-day fields, and suggests that the creation of climatologies is a far more suitable solution than offering daily motion fields at the present time. Mean motion fields were also compared with long-term mean ECMWF pressure and wind fields. Climatological motion fields indicate slight offsets in the locations of synoptic low-pressure centers, raising questions about the quality of geostrophically-forced ice drift velocities inferred from analysis products.

Seasonally-varying Autocorrelation Function

CCAR daily SSM/I velocity statistics have been used to investigate the seasonally varying form of the autocorrelation function. The gridded vector fields were used to compute lagged correlations in the x and y projection directions of the polar stereographic projection for each of the u and v velocity components. An exponential fit to the results provided a method of evaluating the e-folding length scales (L_x , L_y), summarized in the Table below:

U	Jan-Mar	Apr-Jun	Jul-Sep	Oct-Dec
Lx(km)	252.2	319.8	354.1	564.4
Ly(km)	301.4	537.9	755.1	856.9
V				
Lx(km)	291.4	383.8	740.1	717.5
Ly(km)	218.2	401.3	505.8	714.5

Clearly, the e-folding length scale is anisotropic and seasonally dependent. Plots created prior to averaging in the x and y directions also indicate regional dependencies in the length scales, due to the fact that Antarctic sea ice does not simply comprise an annulus. Motion within the two primary Gyre circulations (i.e. in the Weddell and Ross Seas) have different length scales. The above generalized (i.e. Antarctic wide) mean length scales may be applied in optimal analysis schemes which blend the SSM/I vectors with other motion products. However, further analyses of regional dependencies must be investigated to find a solution for generating seamless Southern Ocean wide gridded products, without having to regionally compartmentalize the data for optimal interpolation.

ERS-1 Scatterometer Data

For ERS-1 Scatterometer images, the effective resolution for a stationary target is ~20-25 km, and the gridded pixel spacing 8.9 km (i.e. that imposed by the fine-resolution gridding in the imaging algorithm). The effective resolution in these scatterometer images depends on latitude, sampling considerations and measurement overlap.

Results of ice motion tracking using these data at 3-d intervals show the Scatterometer-derived motions to be aliased due to the irregular sampling intervals over the 6-day temporal averaging period. The result is a relatively poor comparison with Weddell Sea buoy-derived drift. 3-day rms tracking errors were computed relative to the buoy reference displacement vectors in the Weddell Sea, Antarctica, where $\text{error}_{x,y} = \text{buoy}_{x,y} - \text{vector}_{x,y}$. The resulting rms errors are;

- 3 day x displacement error = 2.36 pixels = 21.0 km - or of the order of 9.56 over-sampled pixels (spaced at 2.2km intervals). This is the equivalent of a 7.0 km/d (8.1 cm/s) velocity error.
- 3-day y displacement error = 2.27 pixels = 20.2 km - or of the order of 9.2 over-sampled pixels. This is the equivalent to a 6.73 km/d (7.79cm/s) velocity error.
- Combined 1 day displacement and velocity errors for ERS-1 Scat are 9.7 km/d and 11.22 cm/s, respectively.

Errors in the Weddell Sea indicate that buoys on the shelf respond significantly to tidal currents, and aliasing of the tidal component is an important consideration. Comparisons with 1-day SAR drift confirms the small-scale response to semi-diurnal and diurnal tidal components. Greater high frequency variance in the buoy component of the tidal currents appears to contribute significantly to the underestimation of the motion by the scatterometer. The scatterometer therefore tends to sample the

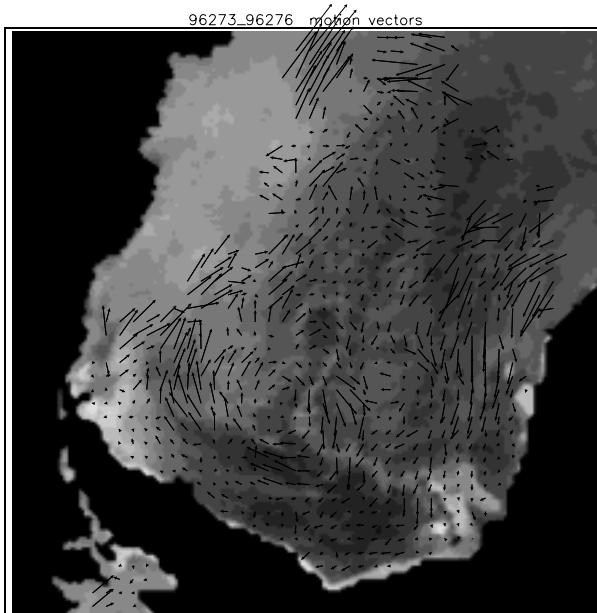


Figure 2. Weddell Sea NSCAT v-pol image from day 273 (29 Sept.), 1996, superimposed by tracked ice-motion vectors for the 3-day period between day 273 and 276 (1 Oct., 1996).

underlying weekly mean ice drift, due to mean synoptic conditions. To-date mainly climatological ERS Scatterometer results have been presented.

NSCAT Ice Motion

In contrast to the ERS Scatterometer images, the NSCAT effective resolution is 8-10 km, and the pixel spacing 4.45 km. This resolution provides much more effective capability to track the NSCAT images. Tracking has been tested in conjunction with Ron Kwok, using these enhanced resolution Antarctic NSCAT image data. A result is shown in Figure 2 for the Weddell Sea quadrant of Antarctica.

So far, the NSCAT data have not been processed for the entire period of the NSCAT mission (i.e. Sept. 1996 - June 1997). Ultimately, when these data are processed, they will be converted into ice motion products. Average NSCAT images appear to be poor at tracking marginal ice drift, particularly regions of pancake ice growth, illustrated by the bright patch in the upper central portion of Figure 2.

Results and Achievements

Dynamically influenced Ice Formation Processes

Weddell Sea ice drift dynamics control to a large extent where ice formation hot spots occur. As Figure 1 indicates, the atmospheric pressure field over the Weddell Sea drives geostrophic ice drift northwards, away from the Ronne-Filchner ice shelf at the southern boundary. Although sea-ice models indicate high ice production in these regions, the actual ice formation process has not been investigated in much detail. SSM/I data do not allow investigations in regions directly abutting the ice shelves because of resolution problems, and ice-shelf overspill.

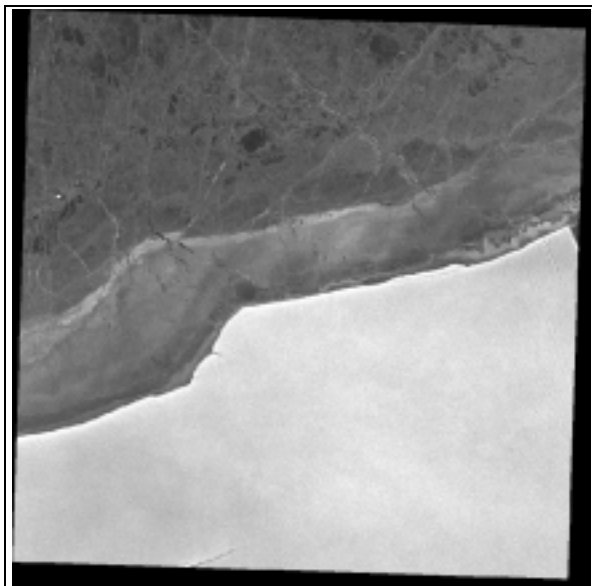


Figure 3. Radarsat Standard Beam 2 image of the Ronne ice shelf margin, from orbit 05040, frame 653. Banding in the sea-ice cover indicates periods where northwards ice drift opens the polynya, inducing new ice formation.

RADARSAT images acquired along the Ronne-Filchner ice shelf indicate frequent and regular periods whereby ice is removed from the shelf-front by northwards drift. The pattern of drift is recorded in the sea-ice conditions, whereby a regular repeating pattern of parallel bands of increasing ice age appear in SAR data (in Figure 3).

Measurements of long-term mean opening and closing made directly using satellite ice kinematics products during the entire year of 1992 indicate that the regional sea-ice cover off the Ronne ice shelf dilates consistently throughout the year. Clearly, temporal variability in wind forcing on short timescales causes periodic opening and closing and abrupt changes in polynya area. Figure 4 shows the result of computing the ice dynamics in the region abutting the Ronne ice shelf from the 1992 SSM/I-derived daily ice motion data. Time-varying results are derived from the partial derivatives of zonal and meridional components of the gridded ice drift field within a study box along the ice-shelf front.

Repeated opening and closing of this ice-shelf polynya provides a convenient mechanism for clearing away (*i.e.* ridging) recently formed ice. This maintains a higher heat flux environment than is possible from linear time-dependent ice growth with slow, constant drift removal, and is the primary mechanism by which active, vigorous ice production is maintained.

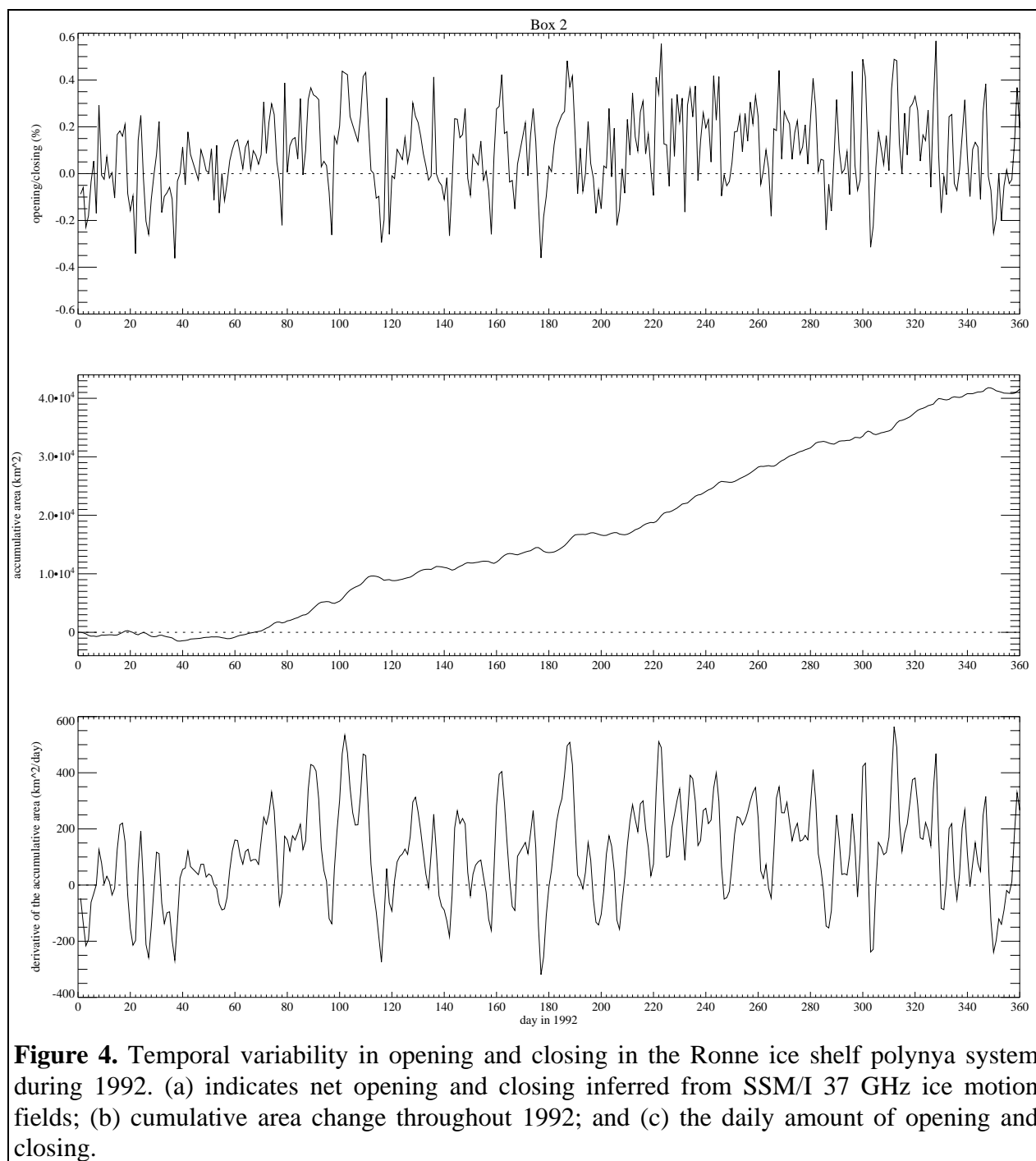


Figure 4. Temporal variability in opening and closing in the Ronne ice shelf polynya system during 1992. (a) indicates net opening and closing inferred from SSM/I 37 GHz ice motion fields; (b) cumulative area change throughout 1992; and (c) the daily amount of opening and closing.

Comparisons between NSCAT and RADARSAT data

RADARSAT data have been selected in the Ross Sea and Weddell Sea basins as training sites for a multi-channel classification scheme being implemented by Quinn Remund at BYU. Polar scatterometer images from NSCAT and ERS-1/2 are being combined with SSM/I to generate

sea-ice classifications on a polar stereographic grid. The channels presently used for the classification are as follows:

- NSCAT (4 channels): Ku-band - hh and vv polarized *A* and *B* images
- ERS-1/2 Scat (2 channels): C-band - vv polarized *A* and *B* images
- SSM/I (7 channels): 19.4 GHz v/h; 22.2 GHz v; 37.0 GHz v,h; 85.5 GHz v,h

Presently we are using co-polarized Ku-band NSCAT data to develop an efficient 4.5 km

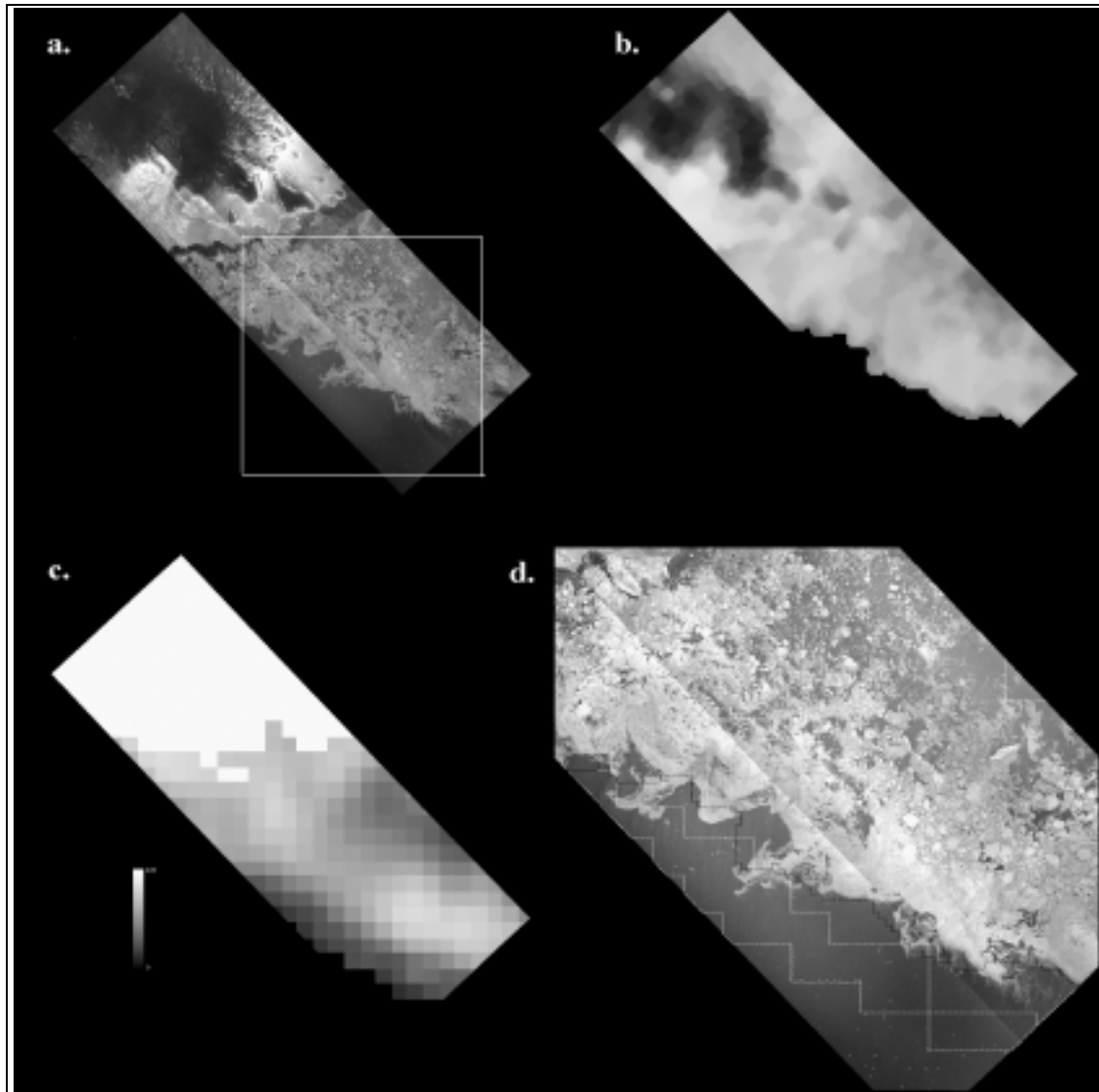


Figure 5. Comparison of (a) Radarsat Wide Swath (SNB) image acquired on day 51, 1997 (20 Feb.) crossing the Ross Sea on orbit 06771; (b) NSCAT vv-polarized normalized backscatter image; (c) 6-day average SSM/I ice concentration image; and (d) zoom of white box region showing comparison between the NSCAT-derived ice edge, and the 15% and 30% ice concentration contours extracted from panel (c).

resolution ice mask for both hemispheres. The hh/vv co-pol ratio is presently employed to define the ocean margin of the sea-ice cover. The NSCAT ice-edge masking result appears to correspond most closely with the 30% SSM/I ice concentration contour. Figure 5 shows a comparison between different summer ice edges, superimposed on a Wide Swath RADARSAT scene from the Ross Sea. Clearly, NSCAT shows the closest approximation to the instantaneous location of the ice margin on 20 February 1997, in this austral summer scene. Both the 15% and 30% SSM/I ice concentration contours appear to indicate a more extensive ice cover than is present during melt retreat. However, the NSCAT image is comprised of data acquired on 6 consecutive days of overlapping orbits, and so in cases where the ice edge is relatively dynamic, comparisons with snap-shot images do not necessarily indicate the validity of the daily SSM/I ice margin locations.

Austral Summer Melt

A preliminary algorithm has been designed to detect the occurrence of melting in the Weddell Sea, using Scatterometer image time-series data. The melt detection algorithm is presently configured to detect an onset of surface melt characterized by an abrupt decline in 40° incidence backscatter coefficient of more than -5 dB, over a contiguous time period exceeding 9 days. The algorithm is presently being validated using a combination of RADARSAT image data and 'in situ' measurements.

To spatially characterize the expression of surface melting, a simple snapshot difference image is generated in Figure 6 to indicate the backscatter contrast between typical winter, 12 November

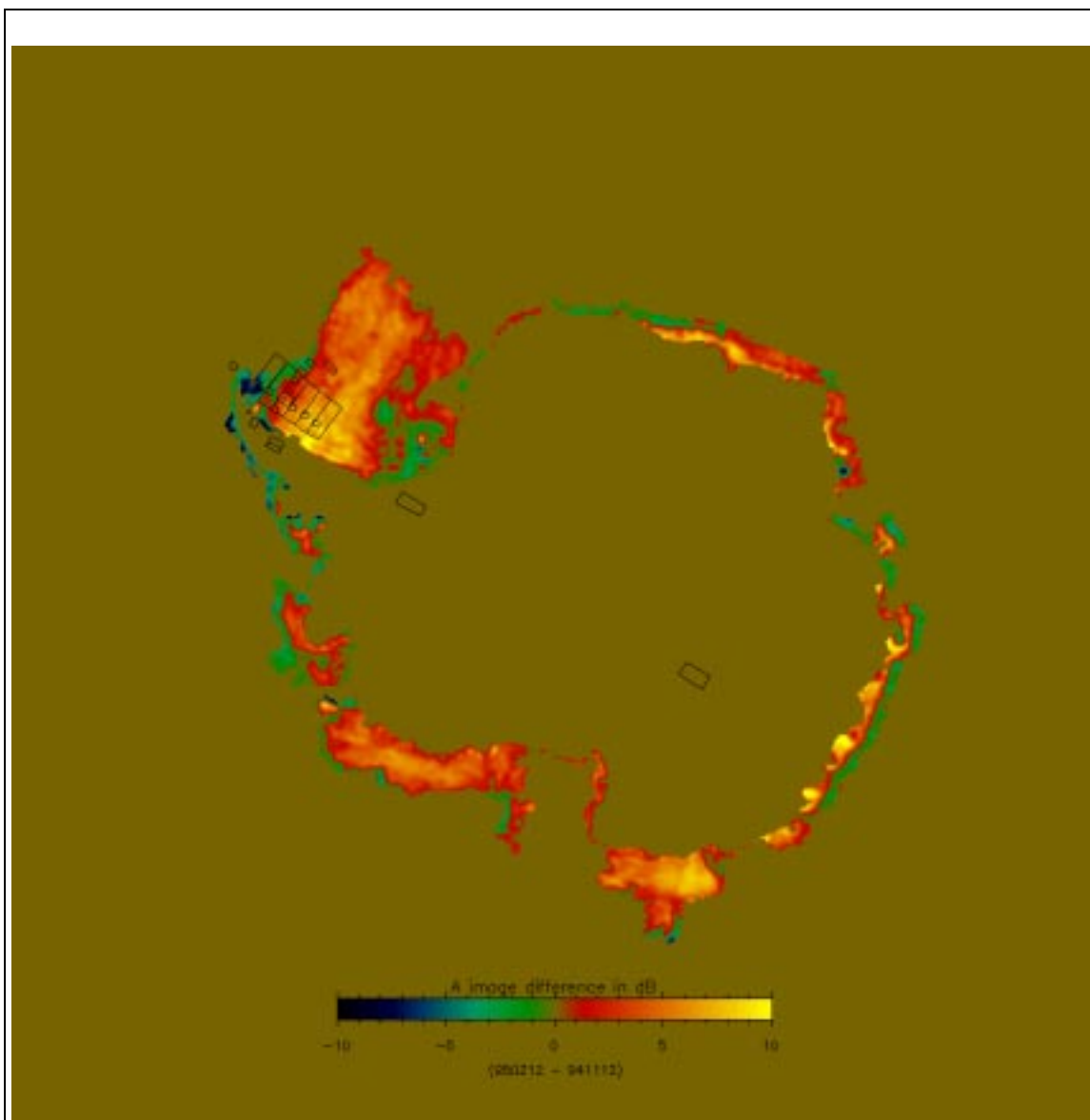


Figure 6. Difference image expressing the typical Antarctic pre-summer (12 November, 1994) and mid-summer melt (12 February, 1995) backscatter contrast in ERS-2 Scatterometer image data. Blue tones indicate a decrease in backscatter due to surface melt, while yellow and red tones indicate summer increases in backscatter in response to flooding. The ice margin is masked using SSM/I ice concentration data.

1994 (*i.e.* pre-melt) and 12 February, 1995, summer conditions (*i.e.* active melting). Blue and green colors indicate negative differences ranging between -10 and 0 dB, while red or orange tones indicate locations where summer backscatter increased. Negative values indicate the widespread occurrence of melting, particularly around the outer ice margin where air temperatures reach their maximum values in summer. Large positive differences are observed to occur in regions with a large perennial ice cover undergoing summer surface flooding (Drinkwater and Lytle, 1997).

Problems

Data Issues

It is presently impossible to tell how many images have been acquired from the Data Acquisition Requests which I placed for my ADRO study. This is not transparent in any of the archives, nor is it evident from the types of products or their regional distribution in the IMS system plots. No feedback is provided from ASF on whether Antarctic RADARSAT scenes have been acquired for an investigator. It would be quite simple to associate a granule of data with a particular investigator whose DAR matches the type of data acquired. Then the catalog could issue an email to all recipients whose DAR requested data of that type.

Some acquired frames delivered from Gatineau have been successfully scanned and appear in the ASF catalog. Others either could not be scanned or processed. A summary of the frames ordered and delivered follows.

ADRO Data Summary

From 126 ordered data frames 35 have been delivered. Of these 35, only 28 frames are SCANSAR images, of which none are calibrated. All ScanSAR data must be reprocessed due to mis-location problems and the required calibration. To-date we have analysed all of the scenes received and made visual/digital comparisons with overlapping scatterometer images. The delivered and analysed frames break-down as follows:

- Std. Beam = 7 frames delivered
- ScanSAR (SNB) = 28 frames delivered
- Total = 35 RADARSAT SAR frames

Geolocation and Calibration Problems

None of these Wide Swath data are calibrated. Geolocation routines work fine, albeit with incorrect earth locations in the metadata. Thus it is presently not possible to use the RADARSAT data for anything to guide the Scatterometer ice classification. Nor is it possible to track sea ice with uncalibrated images, due to the geolocation problems.

To date, ASF Eulerian ice motion processing software is not ready and it is not possible yet to develop ice motion records in Antarctica from the RADARSAT data. A further problem is that

insufficient images were collected at short time intervals for tracking and application to ice dynamics studies.

Future Plans

Out plans are to incorporate calibrated RADARSAT Wide Swath image products into these analyses as soon as they become available for order. We will continue to work with alternative datasets such as Standard Beam RADARSAT images (and ERS-1/2 and JERS-1) data in the absence of unqualified, and non-calibrated scenes.

Since present ASF plans prioritize calibration of the different beam modes used for Wide Swath data acquisitions, we will adjust our Data Acquisition Requests to plan acquisitions using the first qualified and calibrated, tape-recordable Wide Swath mode (i.e. SWB). To-date ScanSAR Narrow B mode (SNB) was used for all Weddell and Ross Sea acquisitions because data volumes are significantly lower, thus facilitating more frequent Antarctic, tape-recorded data takes. It appears that none of these products will be available in calibrated form until summer 1999, and may thus preclude use of any of these products in the scope of the present funded ADRO project.

References and Recent Publications

- Alaska SAR Facility User Working Group, The Critical Role of SAR in Earth System Science, White Paper, Alaska SAR Facility Report, Geophysical Institute, Univ. Alaska Fairbanks, Alaska, June 1998, 46pp., 1998.
- Drinkwater, M.R., Satellite Microwave Radar Observations of Antarctic Sea Ice. In C. Tsatsoulis and R. Kwok (Eds.), *Analysis of SAR Data of the Polar Oceans*, Chapt. 8, 147-187, Springer-Verlag, Berlin, 1998a.
- Drinkwater, M.R., Active Microwave Remote Sensing Observations of Weddell Sea Ice. In M.O. Jeffries (Ed.) *Antarctic Sea Ice: Physical Processes, Interactions and Variability*, *Antarctic Research Series.*, 74, 187-212, American Geophysical Union, Washington, D.C., 1998b.
- Drinkwater, M.R., and X. Liu, Satellite Observations of Southern Ocean Sea-Ice Circulation and Dynamics (OS51B-4), Western Pacific Geophysics Meeting, Taipei, Taiwan 21-24 July, 1998 Eos Transactions, American Geophysical Union, Vol. 79, No. 24, p46, June 16, 1998.
- Drinkwater, M.R., and D.G. Long, Seasat, ERS-1/2 and NSCAT Scatterometer Observed Changes on the Large Ice Sheets, *Proc. IGARSS '98*, Seattle, Washington, 6-10 July, 1998., IEEE Catalog # 98CH36174, Vol. 4, 2252-2254, 1998.
- Drinkwater, M.R., and V.I. Lytle, ERS-1 SAR and field-observed characteristics of austral fall freeze-up in the Weddell Sea, Antarctica, *J. Geophys. Res.*, 102, C6, 12593-12608, 1997.
- Drinkwater, M.R., X. Liu, and D. Low, Interannual Variability in Weddell Sea Ice from ERS Wind Scatterometer, *Proc. IGARSS '98*, Seattle, Washington, 6-10 July, 1998., IEEE Catalog # 98CH36174, Vol. 4, 1982-1984, 1998.

- Eriksson, L., M.R. Drinkwater, B. Holt, E. Valjavek, and O. Nortier, SIR-C Polarimetric Radar Results from the Weddell Sea, Antarctica, *Proc. IGARSS '98*, Seattle, Washington, 6-10 July, 1998., IEEE Catalog # 98CH36174, Vol. 4, 2222-2224, 1998.
- Long, D.G., and M.R. Drinkwater, Cryosphere Applications of NSCAT Data, *IEEE Trans. Geosci. and Remote Sens.*, In Press.
- Massom, R., M.R. Drinkwater and C. Haas, Winter Snowcover on Sea Ice in the Weddell Sea, *J. Geophys. Res.*, 102 (C1), 1101-1117, 1997.
- Remund, Q., D.G. Long, and M.R. Drinkwater, Polar Sea Ice Classification using Enhanced Resolution NSCAT Data, *Proc. IGARSS '98*, Seattle, Washington, 6-10 July, 1998., IEEE Catalog # 98CH36174, Vol. 4, 1976-1978, 1998.
- Stammerjohn, S., R. Smith, M.R. Drinkwater, and X. Liu, Variability in Sea-Ice Coverage and Ice-motion Dynamics in the PAL LTER Study Region West of the Antarctic Peninsula, *Proc. IGARSS '98*, Seattle, Washington, 6-10 July, 1998., IEEE Catalog # 98CH36174, Vol. 3, 1434-1436, 1998.

Budget Explanation

A 1998 NASA Cost Plan is attached which shows the \$152K projected costs for support of research analyst Xiang Liu, requested through this renewal. This funding includes 0% support for the PI, currently supported through SRT research money. As requested, the budget sheet is divided into two columns. The 9 month period 4/1/99 - 12/31/99 is itemized under the FY '99 column, and the final 3 months of year 2000 are itemized under the FY '00 column.

FY '99 - '00 funding is sought to support 100% of analyst Xiang Liu (@ \$52K/yr salaried time); and one networked computer. The latter includes JPL-outsourced hardware and software support, email, networking and 'amortized' hardware replenishment costs (all dictated by the new contract which JPL has negotiated with the company OAO). The level of funding required, including JPL burden and indirect costs is \$152K. JPL 'indirect' and 'burdened' costs total approximately 40% of the bottom-line figure (i.e. ~\$61K indirect costs: or the equivalent of 70% of the direct costs total).